

Simulation of Helicopter Shipboard Launch and Recovery with Time-Accurate Airwakes

Dooyong Lee
Graduate Research
Assistant

Nilay Sezer-Uzol
Graduate Research
Assistant

Joseph F. Horn
Assistant Professor

Lyle N. Long
Professor

*Department of Aerospace Engineering
Pennsylvania State University
University Park, PA USA.*

A simulation of the helicopter/ship dynamic interface has been developed and applied to simulate a UH-60A operating from an LHA class ship. Time accurate CFD solutions of the LHA airwake are interfaced with a flight dynamics simulation based on the GENHEL model. The flight dynamics model was updated to include improved inflow modeling and gust penetration effects of the ship airwake. A maneuver controller was used to simulate pilot control inputs for specified approach and departure trajectories. The CFD solutions show significant time varying flow effects in the airwake. Time histories of the aircraft angular rate and pilot control activity indicate that the time varying nature of the airwake has significant effect on aircraft response and pilot workload.

Introduction

Shipboard launch and recovery is one of the most challenging, training intensive and dangerous of all helicopter flight operations. Ship-based helicopters must operate off rolling and pitching decks, in adverse weather conditions, and often within close proximity to the superstructure of the ship. To ensure the compatibility of a particular rotorcraft and ship under various operating conditions, extensive dynamic interface flight-testing must be performed. This approach is both costly and limited by the availability of fleet assets. Better simulation tools for analyzing shipboard operations might be used to reduce flight test time and cost for establishing safe operating envelopes. Such a simulation tool could be used to find the best approach paths for safe landings, provide improved simulator training for pilots, and ultimately be used in the design or acceptance testing of future rotorcraft and future ships [1]. Furthermore, it could be used to develop new flight control systems to improve handling qualities or even autonomous landing systems.

The wind over deck (WOD) conditions are a very important issue. Disturbances due to the turbulent, unsteady flow field of the ship can have significant effect on pilot workload, and thus the fidelity of the dynamic interface simulation is dependent on an accurate representation of the ship's airwake. A logical

solution is to couple the flight dynamics simulation with time accurate CFD solutions of the ship airwake.

Understanding and modeling the ship airwake presents a number of technical challenges. Complex ship geometries (with superstructures and sharp edges), atmospheric boundary layers, atmospheric turbulence, and helicopter/ship airwake interactions all add to the complexity of the flow field. Some of the key flow features of the airwake are: unsteadiness, large regions of separated flow, vorticity, and low Mach number. Previous researchers have performed numerous experimental and computational studies of airwakes for different classes of ships. The U.S. Navy has done some experimental investigations using both full-scale tests (which are costly and time consuming) and scale-model tests in wind tunnels [2]. Computational simulations of ship airwakes have been performed using different numerical approaches by Tai [3], Tattersall *et al* [4], Liu and Long [5], Guillot and Walker [6], Reddy *et al* [7]. Recently, Sharma and Long [8] have simulated inviscid, steady and time-accurate flow over an LPD-17 ship using a modified parallel flow solver PUMA. They found good agreement between the steady-state solution and frequency spectrum of the wind tunnel experiments. Polsky and Bruner [9, 10] have investigated LHA ship airwakes using the parallel unstructured flow solver COBALT with different numerical methods such as laminar Navier-Stokes and MILES as well as $k-\omega$ and SST turbulence modeling. It was shown that steady-state CFD calculations were unable to predict the time average of the turbulent flow field, and observed that turbulence modeling added too much dissipation to the calculation since the flux-splitting numerical schemes are very dissipative. Bogstad *et al* [11] have solved for

inviscid flow around six different ships of the Royal Navy to obtain an airwake database for a helicopter flight simulator (Merlin). Camelli *et al* [12] have performed an LES simulation of airwake and stack gas temperature field around the LPD-17 class ship using a Smagorinsky turbulence model.

A number of recent research programs have also focused on the simulation of helicopter flight dynamics during shipboard operations, with the goal of assessing handling qualities and pilot workload. The Joint Shipboard Helicopter Integration Process (JSHIP) has been applied to increase the interoperability of joint shipboard helicopter operations for helicopters that are not specifically designed to go aboard Navy ships [13,14,15]. JSHIP is evaluating the compatibility, and procedures and training issues associated with integrating ARMY and Air Force helicopters with Navy ships. As a part of JSHIP, the Dynamic Interface Modeling and Simulation System (DIMSS) was established to define and evaluate a process for developing WOD flight envelopes. Using DIMSS, the fidelity standards for the shipboard launch and recovery task has been discussed for combination of an LHA class ship and a UH-60 [14]. The UCE (Useable Cue Environment) determination test methods have been discussed for the same combination of ship and helicopter [15]. The helicopter shipboard operational limit prediction tool with coupled helicopter/ship aerodynamic interaction and integrated flight envelope analysis have been studied by He, et al [16]. Inverse simulation techniques have also been applied to determine the pilot control input for shipboard launch and recovery operations [17]. Bradley and Turner have investigated the crossover model to represent the pilots reflexive actions in terms of simple gain and delay parameters [18].

In this study, a dynamic interface simulation of the UH-60A helicopter operating off an LHA is developed. This represents the same aircraft ship combination used in the JSHIP program. The objective of this study is to understand the impact of a time-varying ship airwake on the pilot control activity for approach and departure operations. The model builds upon a previous analysis of the UH-60 operating near a generic frigate [19]. In that study, steady-state CFD solutions of the frigate airwake were coupled with an experimentally derived stochastic representation of the time-varying airwake [20]. The time-varying component of the airwake was assumed to be uniform over the entire body of the aircraft. In this study, the model of the helicopter / ship dynamic interface is modified to include time accurate solutions of the ship airwake. The Parallel Unstructured Maritime Aerodynamics CFD solver (PUMA2) is used to calculate the flow over the LHA. Both the temporal and spatial variation of the unsteady wake are accounted for

in the flight dynamics simulation. A maneuver controller is used to simulate the pilot control inputs required to perform approach and departure operations, and the qualitative effects of time varying ship airwake on pilot control activity are explored. The results show that the unsteadiness of the ship airwake has significant impact on pilot workload when the helicopter is operating near the deck and superstructure of the ship.

Helicopter/Ship Dynamic Interface Simulation Model

To simulate the helicopter/ship dynamic interface, it is necessary to model the kinematics, dynamics, and aerodynamics of the helicopter, the flight control system, the ship motion, and the airwake of the ship. The focus of this study is on the affect of airwake, and the ship motion due to sea state is not modeled. The flight dynamics model is based on the GENHEL model of the UH-60A [21]. To facilitate model improvements and control law development, a MATLAB/SIMULINK based version is developed (Figure 1). The code has been updated to include a high order Peters-He inflow model with moving ground effects [22,23], and a special gust penetration model is developed to include the effects of ship airwakes. Time accurate CFD solutions of the LHA are used to provide both steady-state and time-varying airwake velocities that result in local gust disturbances at various locations on the helicopter. The gust penetration model extends previous research on ship airwake and atmospheric turbulence disturbances on helicopters [20,24,25]. In order to simulate approach and departure trajectories, a maneuver controller has been developed [19]. This controller is used to simulate specified approach and departure trajectories in order to analyze pilot control activity.

Ship Airwake Model – CFD Flow Solver

The helicopter simulation is integrated with time-accurate CFD solutions of the airwake of an LHA class ship. The Parallel Unstructured Maritime Aerodynamics CFD solver (PUMA2) is used to calculate the flow. It uses a finite volume formulation of the Euler/Navier-Stokes equations for 3-D, internal and external, non-reacting, compressible, steady/unsteady solutions for complex geometries. PUMA2 can be run so as to preserve time accuracy or as a pseudo-unsteady formulation to enhance convergence to steady state. It is written in ANSI C using the MPI library for message passing so it can be run on parallel computers and clusters. It is also compatible with C++ compilers and coupled with the computational steering system POSSE [26]. It uses dynamic memory allocation, thus the problem size is limited only by the amount of memory

available on the machine. Large eddy simulations can also be performed with PUMA2. [26,27].

Helicopter Flight Dynamic Model

The overall structure of the GenHel model is presented in Figure 1. The simulation model is divided into sub-modules that represent the aerodynamics and dynamics of various aircraft components (e.g. main rotor, fuselage, empennage, tail rotor). The total forces and moments are calculated from a sum of the aerodynamic, mass and inertia forces acting on each component. The simulation uses a total force, large angle representation of the six rigid body degrees of freedom of the fuselage. The main rotor module includes rigid rotor blade flapping, lagging, and rotational degrees of freedom as well as an air mass degree of freedom. In this study, the model was updated to include a high order Peters-He inflow model.

This Peters-He inflow model is based on an acceleration potential with a skewed cylindrical wake. The flow field and the rotor lift are expanded in terms of appropriate inflow modes. The induced flow is expressed azimuthally by a Fourier series and radially by Legendre functions. The magnitude of each term is determined from first order ordinary differential equations in either the time or frequency domain, with blade lift as the forcing function [22]. In this paper, a 15 state inflow model is used.

The flight control system consists of the primary mechanical flight control system and the Automatic Flight Control System (AFCS). The AFCS includes the Stability Augmentation System (SAS), the Pitch Bias Actuator (PBA), the Flight Path Stabilization (FPS), and an automatic Stabilator. An analytical definition of the control system is given in Ref. [21].

Gust Penetration Model

The gust penetration model is used to model the effects of a three-dimensional ship airwake. For the distribution of the gust velocities over the helicopter, the velocity field is determined at all of the distributed components on the helicopter (Figure 2). Thus the location of all of the components must be computed at each point in time relative to the ship. To account for local velocities at the rotor blade elements, fuselage, empennage and tail rotor, a 3-dimensional interpolation algorithm is applied. The ship airwake velocity field provided by the CFD database is defined with respect to a ship-fixed coordinate system. Thus, the velocity field must be transformed to inertial axes, and then to the specific axis systems used for each of the helicopter component models. For the fuselage, empennage and tail rotor, the following coordinate transformation is required.

$$\vec{V}_{body} = \mathbf{T}_{i2b} \mathbf{T}_{s2i} \vec{V}_{ship} \quad (1)$$

where, \vec{V}_{ship} is the ship wake velocity in ship coordinate system, \vec{V}_{body} is the ship wake velocity in the helicopter body coordinate system, \mathbf{T}_{s2i} is the coordinate transformation matrix from ship coordinate system to inertial coordinate system and \mathbf{T}_{i2b} is the coordinate transformation matrix from inertial to helicopter body coordinate system.

For each main rotor blade element, a more complicated coordinate transformation is required.

$$\vec{V}_{rotor} = \mathbf{T}_{h2b} \mathbf{T}_{b2h} \mathbf{T}_{i2b} \mathbf{T}_{s2i} \vec{V}_{ship} \quad (2)$$

where, \vec{V}_{rotor} is the ship wake velocity in blade coordinate system, \mathbf{T}_{b2h} is the coordinate transformation matrix from helicopter body to hub coordinate system, \mathbf{T}_{h2b} is the coordinate transformation matrix from hub to each blade coordinate system. These transformations must account for the orientation of the helicopter, the hub, and all of the rotor degrees of freedom.

The time-varying components of the airwake are stored at every 0.1 seconds for a total of 20 seconds of time history. Linear interpolation is used to calculate the gust field at every simulation time step (0.01 seconds). Since the maneuvers generally last longer than 20 seconds, the whole time accurate flow solutions must be repeated. After 20 seconds, the solutions are loaded in reverse order to prevent the sudden jumps. This algorithm is presented in Figure 3.

Maneuver Controller

The control of a helicopter is a genuinely multivariable problem in which one must consider at least four inputs and four outputs with significant inter-axis coupling. There have been a number of studies on robust, multivariable flight controller design for modern helicopters. [28-30]. In this study, we are interested in the multi-axis control of the helicopter in order to simulate specified approach and departure trajectories. Thus, by studying the time history of the control inputs, some knowledge of pilot control activity and workload can be assessed. In the past, inverse simulation methods have been used to calculate pilot control inputs for specified trajectories. Inverse simulation methods can be generally divided into two categories, the differentiation-based inverse method and integration-based inverse method [16,17]. Both inverse simulation methods have certain disadvantages such as computational expense and solution inaccuracy for a long time period. A more efficient approach is to apply modern control theory to design an outer loop controller to achieve our desired trajectory.

The control system structure used in this paper is shown in Figure 4. A simple PID control structure is used. To find suitable gains for this controller, a set of linearized models are derived from GENHEL. The linear, time-invariant mathematical model used in this paper is obtained through numerical linearization about a trimmed flight condition. The linear model has a total of 29 states, of which 9 define the body motion and 18 define the flap, lag motion and rotor inflow. In addition, main rotor RPM degree of freedom servo dynamics and engine-governor dynamics are included. The design approach begins with model order reduction. First, power plant states are removed with assumption of constant rotor speed. The main rotor flapping, lagging and inflow states are removed with the assumption of a quasi-steady rotor. This results in a 9 state / 6 DOF model of the rigid body motion of the helicopter. The model is then decoupled into longitudinal and lateral dynamics where the decoupled systems are described by:

$$\begin{aligned}\dot{\mathbf{x}}_{long} &= \mathbf{A}_{long} \mathbf{x}_{long} + \mathbf{B}_{long} \mathbf{u}_{long} \\ \dot{\mathbf{x}}_{lat} &= \mathbf{A}_{lat} \mathbf{x}_{lat} + \mathbf{B}_{lat} \mathbf{u}_{lat}\end{aligned}\quad (3)$$

In the hover flight condition the linear model is given by:

$$\begin{aligned}\mathbf{x}_{long} &= [u \quad w \quad p \quad \theta]^T \\ \mathbf{u}_{long} &= [\delta_{long}] \\ \mathbf{A}_{long} &= \begin{bmatrix} -0.05 & -0.01 & 14.7 & -32.5 \\ -0.3 & -0.3 & 1.3 & -9.6 \\ -0.006 & 0.002 & -4.7 & 0.06 \\ 0 & 0 & 1.0 & 0 \end{bmatrix} \\ \mathbf{B}_{long} &= [-1.5 \quad -0.2 \quad 0.4 \quad 0]^T \\ \mathbf{x}_{lat} &= [v \quad p \quad r \quad \phi \quad \psi]^T \\ \mathbf{u}_{lat} &= [\delta_{lat} \quad \delta_{ped}]^T \\ \mathbf{A}_{lat} &= \begin{bmatrix} -0.07 & -1.04 & 6.6 & 31.5 & 2.4 \\ -0.04 & -7.3 & 2.7 & -2.3 & 1.3 \\ 0.01 & -0.6 & -2.9 & -0.4 & -0.2 \\ 0 & 1.0 & 0.1 & 0 & 0 \\ 0 & 0 & 1.0 & 0 & 0 \end{bmatrix} \\ \mathbf{B}_{lat} &= \begin{bmatrix} 0.47 & -1.01 \\ 1.36 & -0.48 \\ 0.09 & 0.45 \\ 0 & 0 \\ 0 & 0 \end{bmatrix}\end{aligned}\quad (4)$$

The feedback gain matrices can be calculated using the pole-placement method. The results are as follows,

$$\begin{aligned}K_{long} &= [-0.99 \quad 0.17 \quad 4.19 \quad 22.8] \\ K_{lat} &= \begin{bmatrix} 1.88 & 4.73 & 5.54 & 35.6 & 5.6 \\ -0.28 & 4.52 & -0.7 & 6.9 & 4.03 \end{bmatrix}\end{aligned}\quad (5)$$

The control inputs are given as

$$\begin{aligned}\mathbf{u}_{long} &= K_{long} \Delta \mathbf{x}_{long} + K_{long}^I \int \Delta \mathbf{x}_{long} + K_{long}^D \frac{d}{dt} \Delta \mathbf{x}_{long} \\ \mathbf{u}_{lat} &= K_{lat} \Delta \mathbf{x}_{lat} + K_{lat}^I \int \Delta \mathbf{x}_{lat} + K_{lat}^D \frac{d}{dt} \Delta \mathbf{x}_{lat} \\ \mathbf{u}_{col} &= K_{col} \Delta \mathbf{x}_{col} + K_{col}^I \int \Delta \mathbf{x}_{col} + K_{col}^D \frac{d}{dt} \Delta \mathbf{x}_{col}\end{aligned}\quad (6)$$

Note an additional controller is applied to the heave axis where $\Delta \mathbf{x}_{col} = [w]$, in order control vertical speed. The corresponding integral and derivative controller parameters are selected so that the total requirement on relative stability is satisfied.

Shipboard Operations

In this study, typical shipboard approach and departure trajectories are simulated. Kinematical profiles of these shipboard tasks are given in Ref. [17], and these profiles are modified slightly in this study. The kinematical profile is determined using an Earth fixed coordinate frame with the origin at the sea surface directly under the initial position of the helicopter. The X-axis is along with the North direction, Z-axis is downward, and Y-axis is along with the East direction. In this study, simple one-dimensional motion of the ship is considered (in the X direction only). The shipboard approach and departure spot is spot 8 of the LHA class ship (Figure 5).

Typical shipboard approach procedures include all actions that bring the rotorcraft from a point far away from the ship down to a point much closer to the recovery spot [13,17]. The development of the kinematics profile for a shipboard approach is presented in Ref. [19]. The entire shipboard approach task can be divided into three phases:

1. Phase I: From steady level flight, the helicopter transitions to a desired descent rate and horizontal deceleration.
2. Phase II : The helicopter maintains a constant descent rate and horizontal deceleration.
3. Phase III : The descent rate and horizontal deceleration are reduced to zero, ending in station-keeping over a landing spot.

The key parameters for defining the approach profile are the helicopter initial level flight speed, initial altitude,

initial distance from the ship, and desired final altitude for stationkeeping. In this study it is assumed that the helicopter approaches the ship at a 45 deg angle, and the ship is stationary in a 30 knot headwind.

Typical shipboard departure procedures include all actions that are required to conduct an ascending, acceleration from station-keeping, ending in steady, level forward flight [13,17]. Similar to the approach case, departure task can be divided into three phases. Starting from the stationkeeping location, pilots typically initiate the departure phase by yawing and/or translating the helicopter at a relatively constant altitude to a position outboard of the recovery spot that is clear of obstructions. The helicopter then transitions to a desired climb rate and horizontal acceleration. Finally, the helicopter achieves desired level flight speed. In this study, the departures are performed with the ship moving at 10 knots into a 20 knot headwind.

Simulation Results

CFD Simulation of Ship Airwake

In this study, the simulation model is interfaced with steady-state and time-accurate inviscid CFD predictions for an LHA ship airwake. Figure 6 shows the 3-D unstructured grid for the full-scale LHA geometry, which is generated using the GRIDGEN software. The rectangular computational grid has 854,072 cells. The flow case represents 0 degree yaw angle and Mach number of 0.18 (30 knot of relative wind speed). This is the same case simulated by Polsky and Bruner [9]. A 4-stage Runge-Kutta explicit time integration algorithm with Roe's flux difference scheme is used with CFL numbers of 2.5 and 0.8 for the steady and unsteady computations, respectively. A zero-normal-velocity boundary condition is applied on the ship surface and water surface (bottom surface of the domain) and a Riemann boundary condition is applied at all other faces of the domain. The pseudo steady-state computations are performed using local time-stepping and initialized with freestream values. The time accurate computations are started from the pseudo steady state solution, and the simulation time step (44 μ seconds) is determined by the smallest cell size in the volume grid. The computations are performed on a parallel PC cluster (COCOA-2) consisting of 40 800 MHz Pentium III processors and 20 GB RAM. It takes nearly 22870 iterations to simulate 1 second of real flow (~2 days on 40 processors) with the current grid.

The time-accurate CFD solutions result in large quantities of time history data that need to be mapped into the DI simulation gust penetration model. Thus, for a given launch or recovery operation, the velocity data can be mapped into a rectangular grid (to allow easy table look up) and stored for only that part of the ship

where the aircraft is expected to fly. Figure 7 shows the rectangular volumetric domain of CFD data over the rear deck of LHA for DI simulations and the velocity magnitude contours on the boundaries of the DI mesh which has (52x41x22) grid points with 5ft equal intervals. The DI mesh is selected to have the flow data over the landing spots of 8 and 9. Helicopter enters the DI mesh from the back surface and escapes from it through the front surface according to the calculated approach and departure trajectories. A total of 20 seconds of time-accurate flow solution is obtained and the time history data is stored for every 0.1 seconds to be used for the DI simulations. Each flow solution file is 41 MBytes in size, whereas the DI velocity data is only 4.4 Mbytes.

Figure 8 shows the velocity magnitude contours at several y-z planes over the LHA at the simulation time of 20 seconds. An iso-surface of vorticity magnitude and vorticity contours at several y-z planes over the LHA are shown in Figure 9. Similar features can be observed as in Ref 9 such as bow separation, deck-edge vortices, burbles in the flow field between the bow separation and the island, complex island wake. Figure 10 (a) shows time histories of u, v, w velocity components at a selected point in the DI mesh over landing spot 8. The x,y,z coordinates of the selected point is (-58.02, -20, 74.13) ft. The velocity data at that point is extracted from the 20 seconds of real flow solutions with 0.1 seconds of intervals. The frequency spectrum of the velocity magnitude, which is calculated using FFT function in MATLAB, is plotted in Figure 10 (b). It can be seen that CFD predicts the dominant frequencies to be between 0.1-0.5 Hz, which corresponds to Strouhal numbers of 1.3-6.6 (calculated using the ship length and freestream velocity). Figure 11 shows the distribution of the u, v, w velocity components along the length of LHA at a height of 74.13 ft from the sea level (21.23 ft above the deck) and velocity magnitude contours in a y-z plane at x = -58.02 ft for three different simulation times of 10, 15, 20 seconds over the landing spot 8.

Dynamic Interface Simulation Results

The dynamic interface flight dynamics model has been applied to simulate the UH-60 operating near an LHA class ship. In this case, the helicopter/ship dynamic interface simulation has been performed for three different airwake conditions (no airwake, steady-state airwake, time-varying airwake). The maneuver controller was used to determine the required pilot control inputs for shipboard approach and departure tasks. For the departure operation, the ship was moving forward at 10 knots with a steady-state bow wind of 20 knots. In order to clear obstructions, the departure begins with a 55 ft lateral translation maneuver to the

left (port side). For the approach case, the ship is assumed to be still with a steady-state bow wind of 30 knots. The helicopter approaches the landing spot at a 45 deg angle. The general profile parameters of the shipboard departure are shown in Table 1.

Table 1. Initial profile parameters

	Approach	Departure
Initial Altitude	300ft	70 ft (17ft above deck)
Final Altitude	70 ft	300 ft
Initial Speed	60 knots	10 knots
Final Speed	0 knots	60 knots

Figures 12-17 show the simulation results for the departure operation. The dotted lines represent the no airwake case, the dashed lines represent the steady airwake case, and the solid lines represent the time-varying airwake case. The helicopter trajectory with respect to the ship coordinate system is shown in Figure 12. Figure 13 shows the helicopter velocity in the NED (North-East-Down) coordinate system. Figures 14-15 show the helicopter angular rate and attitude response. The pilot stick inputs provided by the maneuver controller are shown in Figures 16-17. The conventions for these control positions are as follows; full left lateral cyclic, full forward longitudinal cyclic, full down collective pitch, and full left pedal correspond to 0%, full right lateral cyclic, full aft longitudinal cyclic, full up collective pitch, and full right pedal correspond to 100%. The results show that the helicopter trajectory and velocities are very similar in each case. This is because the maneuver controller is regulating these parameters. In effect these variables are constrained to follow the specified trajectory; the maneuver controller is effectively calculating the control inputs and aircraft attitude required to track this trajectory. However, when the helicopter is operating within the DI mesh, there are significant differences in the aircraft angular rates and the pilot control positions for the different airwake cases. The steady airwake results differ only slightly from the results with no airwake in that the trimmed controls and attitude are slightly different, but the time varying nature of the control motion is similar in each case. On the other hand, the time-varying airwake results in significant oscillations and pilot control activity, particularly when hovering over the ship deck. This difference in the results with the steady and time varying airwake was not entirely expected, since a stationary gust field can appear to be time-varying to the aircraft when it is moving (and especially to the rotor blades which are constantly moving).

Figures 18-23 show similar simulation results for the approach operation. Again, it can be observed that there are significant differences in the angular rate and pilot control activity in each of the cases. In this case the aircraft also experiences significant velocity fluctuations in the case of the time-varying wake when it approaches hover. The maneuver is more challenging in this case as the aircraft is operating at a 45 deg angle to the relative wind. In the approach flight, it can also be observed that the oscillations immediately after entering the DI mesh are similar for the steady and time-varying airwake. At this point, the aircraft is still moving with significant velocity so the steady gust field has a time varying appearance to the aircraft. However, once the aircraft approaches hover, the results show that the steady airwake is inadequate for predicting pilot control activity.

From the results, the maneuver controller is reasonably effective in tracking the desired flight path for both approach and departure operations, and thus the trajectories are similar for each of the airwake cases. It is quite apparent that the time-varying ship airwake can have a very significant for helicopter/ship dynamic interface simulation, in that the pilot control response to maintain these trajectories is significantly different. The time varying nature of the airwake would appear to increase pilot workload and thereby degrade handling qualities during shipboard launch and recovery operations.

Conclusions

A helicopter/ship dynamic interface simulation tool has been developed to model a UH-60A operating off an LHA class ship. To achieve a high fidelity simulation model, time-accurate ship airwake solutions of an LHA class ship are integrated with the flight dynamics simulation model. These ship airwake solutions are calculated using PUMA2. Both steady-state and time-accurate inviscid ship airwake flow fields are calculated for the 3 dimensional full-scale LHA geometry. Approach and departure trajectories were simulated from landing spot 8 on the LHA. (CFD results showed significant time-varying flow effects over this spot). Results with no ship airwake, steady airwake, and time-varying airwake were compared. The following conclusions can be made:

1. The results clearly indicate that time-varying airwake has a significant impact on aircraft response and pilot control activity when the aircraft is flown for specified approach and departure trajectories. The differences are most notable when the helicopter is operating in or near a hover relative to the ship deck (stationkeeping). In the

past, gust models for fixed-wing simulation models have used a stationary or frozen field gust model. This is adequate when the aircraft is moving at a significant forward speed. However, the model clearly breaks down as airspeed approaches zero. The same appears to be true of helicopters operating in turbulent ship airwakes. The time-varying nature of the ship airwake becomes dominant as the helicopter approaches a hover relative to the ship deck.

2. A maneuver controller was successfully implemented to solve the "inverse simulation" problem. Given a specified trajectory, the pilot controls can be calculated using forward simulation in conjunction with a feedback controller. This was found to be highly useful for this research task. Inverse simulations can be time consuming and difficult to implement computationally. The maneuver controller, which was designed based on pole placement methods, was found to be effective with relatively little tweaking. A high quality linear model is necessary for implementing this controller.
3. The use of time-accurate ship airwake data was found to present some practical implementation difficulties, as the method requires that the simulation handle large quantities of data. For every grid point a set of time history data must be stored for each component of velocity. Memory storage can become an issue, particularly if the simulations are to be run in real-time, in which case accessing data from disk storage may not be feasible. It was helpful to select a subset of the flowfield when performing the simulations in which the landing spot is known. However, for real-time simulations the pilot might want to access different deck spots during the same simulation run. The use of stochastic airwake model (based on the time accurate CFD results) might be an attractive alternative.
4. The UH-60A / LHA combination of aircraft and ship were selected in part, because a large quantity of flight test data has been collected in the JSHIP program and has been used for limited validation in past dynamic interface simulation studies [14]. It was not possible to obtain the flight data from the JSHIP program for this study, but it is hoped that some data can be obtained in the near future to help validate the model. It would be also relatively simple to modify the simulation to represent a Navy version of the H-60 (SH-60B / SH-60F / SH-60R).

References

1. Mello, O.A.F., Prasad, J.V.R. and Sankar, L.N., Tseng, T., "Analysis of Helicopter/Ship Aerodynamic interactions," The American Helicopter Society Aeromechanics Specialists Conference, San Francisco, CA, January 19-21, 1994.
2. Zan, S.J., Syms, G.F., and Cheney, B.T., "Analysis of Patrol Frigate Air Wakes," Presented at the NATO RTO Symposium on Fluid Dynamics Problems of Vehicles Operating near or in the Air-Sea Interface, Amsterdam, The Netherlands, October 5-8, 1998.
3. Tai, T.C., "Simulation and Analysis of LHD Ship Airwake by Navier-Stokes Method," Presented at the NATO RTO Symposium on Fluid Dynamics Problems of Vehicles Operating near or in the Air-Sea Interface, Amsterdam, The Netherlands, October 1998.
4. Tattersall, P, Albone, C M, Soliman, M M, Allen, C B, "Prediction of Ship Air Wakes over Flight Decks using CFD," In AGARD Fluid Dynamics Symposium on Fluid dynamics of Vehicles Operating Near or In the Air-Sea Interface, Paper No.6, Amsterdam, October 1998.
5. Liu, J. and Long, L.N., "Higher Order Accurate Ship Airwake Predictions for the Helicopter-Ship Interface Problem," Presented at AHS 54th Annual Forum, Washington D.C., May 20-22, 1998.
6. Guillot, M.J., Walker, M.A., "Unsteady Analysis of the Air Wake over the LPD-17," AIAA Paper 2000-4125, AIAA Applied Aerodynamics Conference and Exhibit, 18th, Denver, CO, Aug. 14-17, 2000.
7. Reddy, K.R., Toffoletto, R., Jones, K.R.W., "Numerical simulation of ship airwake," *Computers and Fluids*, Vol29, p451-465, 2000.
8. Sharma, A. and Long, L.N., "Airwake simulations on an LPD 17 ship," AIAA Paper 2001-2589, AIAA Computational Fluid Dynamics Conference, 15th, Anaheim, CA, June 11-14, 2001.
9. Polsky, S. A., Bruner, C. W. S., "Time-Accurate Computational Simulations of an LHA Ship Airwake," *AIAA Paper 2000-4126*, 18th *AIAA Applied Aerodynamics Conference*, Aug. 14-17, 2000, Denver, CO.
10. Polsky, S.A., "A Computational Study of Unsteady Ship Airwake," AIAA Paper 2002-1022, 40th AIAA Aerospace Sciences Meeting & Exhibit, Reno, Nevada, January 14-17, 2002.
11. Bogstad, M.C., Habashi, W.G., Akel, I., Ait-Ali-Yahia, D., Giannias, N., and Longo, V., "Computational-Fluid-Dynamics Based Advanced Ship-Airwake Database for Helicopter Flight Simulators," *Journal of Aircraft*, Vol.39, No.5, September-October 2002.

12. Camelli, F.E., Soto, O., Lohner, R., Sandberg, W.C., and Ramamurti, R., "Topside LPD17 Flow and Temperature Study with an Implicit Monolithic Scheme," AIAA Paper 2003-0969, 41st AIAA Aerospace Sciences Meeting & Exhibit, Reno, Nevada, January 6-9, 2003.
13. Wilkinson, C. and Roscoe, M.F., "DIMSS - JSHIP's Modeling and Simulation Process for Ship/Helicopter Testing and Training," AIAA Paper 2002-4597, AIAA Modeling and Simulation Technologies Conference and Exhibit, Monterey, CA, Aug. 5-8, 2002.
14. Wilkinson, C.H., Roscoe, M.F. and VanderVliet, G.M., "Determining Fidelity Standards for the Shipboard Launch and Recovery Task," AIAA Paper 2001-4062, AIAA Modeling and Simulation Technologies Conference and Exhibit, Montreal, Canada, Aug. 6-9, 2001.
15. Roscoe, M.F., Wilkinson, C.H. and VanderVliet, G.M., "The Use of ADS-33D Useable Cue Environment Techniques for Defining Minimum Visual Fidelity Requirements," AIAA Paper 2001-4063, AIAA Modeling and Simulation Technologies Conference and Exhibit, Montreal, Canada, Aug. 6-9, 2001.
16. He, C., Kang, H., Carico, D. and Long, K., "Development of a Modeling and Simulation Tool for Rotorcraft/Ship Dynamic Interface Testing," American Helicopter Society 59th Annual Forum, Montreal, Canada, June 11-13, 2002.
17. Xin, H. and He, C., "A Combined Technique for Inverse Simulation Applied to Rotorcraft Shipboard Operations," American Helicopter Society 58th Annual Forum, Montreal, Canada, June 11-13 2002.
18. Bradley, R. and Turner, G., "Simulation of the Human Pilot applied at the Helicopter/Ship Dynamic Interface," American Helicopter Society 55th Annual Forum, Montreal, Canada, May 1999,
19. Lee, D. and Horn, J.F., "Simulation and Control of Helicopter Shipboard Launch and Recovery Operations", American Helicopter Society Flight Controls and Crew System Design Specialists' Meeting, Philadelphia, PA, USA, October 9-11, 2002.
20. Labows, S.J., Tischler, M.B. and Blanken, C.L. "UH-60 Black Hawk Disturbance Rejection Study for Hover/Low Speed Handling Qualities Criteria and Turbulence Modeling," The American Helicopter Society 56th Annual Forum, Virginia Beach, Virginia, May 2-4, 2000.
21. Howlett, J.J., "UH-60A BLACK HAWK Engineering Simulation Program: Volume I – Mathematical Model", NASA CR-177542, USAAVSCOM TR 89-A-001, September 1989.
22. He, C., "Development and Application of a Generalized Dynamic Wake Theory of Lifting Rotors," Ph.D. Thesis, School of Aerospace Engineering, Georgia Institute of Technology, Jul 1989.
23. Xin, H., Prasad, J.V.R., and Peters, D., "Dynamic Inflow Modeling for Simulation of a Helicopter Operating in Ground Effect," AIAA Paper 99-4114, AIAA Modeling and Simulation Technologies Conference, Portland, OR, Aug. 9-11, 1999.
24. Dahl, H.J. and Faulkner, A.J., "Helicopter Simulation in Atmospheric Turbulence," 4th European Rotorcraft Forum, Stresa, Italy, Sep. 1978.
25. Clement, W.F., Gorder, P.J. and Jewell, W.F., "Development of a Real-Time Simulation of a Ship-Related Airwake Model Interfaced with a Rotorcraft Dynamic Model," The Naval Air Systems Command, TR-91-C-0176, 1991.
26. Modi, A., Sezer-Uzol, N., Long, L. N., and Plassmann, P. E., "Scalable Computational Steering System for Visualization of Large-Scale CFD Simulations," AIAA Paper 2002-2750, 32nd AIAA Fluid Dynamics Conference and Exhibit, 24–27 June 2002, St. Louis, Missouri.
27. Souliez, F.J., "Parallel Methods for the Computation of Unsteady Separated Flows Around Complex Geometries," *PhD Thesis, Dept. of Aerospace Engineering, The Pennsylvania State University*, August 2002.
28. Takahashi, M.D., "Rotor-State Feedback in the Design of Flight Control Laws for a Hovering Helicopter," *Journal of the American Helicopter Society*, January 1994.
29. Ingle, S.J. and Celi, R., "Effects of Higher Order Dynamics on Helicopter Flight Control Law Design," American Helicopter Society 48th Annual Forum, Washington D.C., June 1992.
30. Trentini, M. and Pieper, J.K., "Mixed Norm Control of a Helicopter," *Journal of Guidance, Control, And Dynamics*, Vol.24, No.3, May-June 2001.

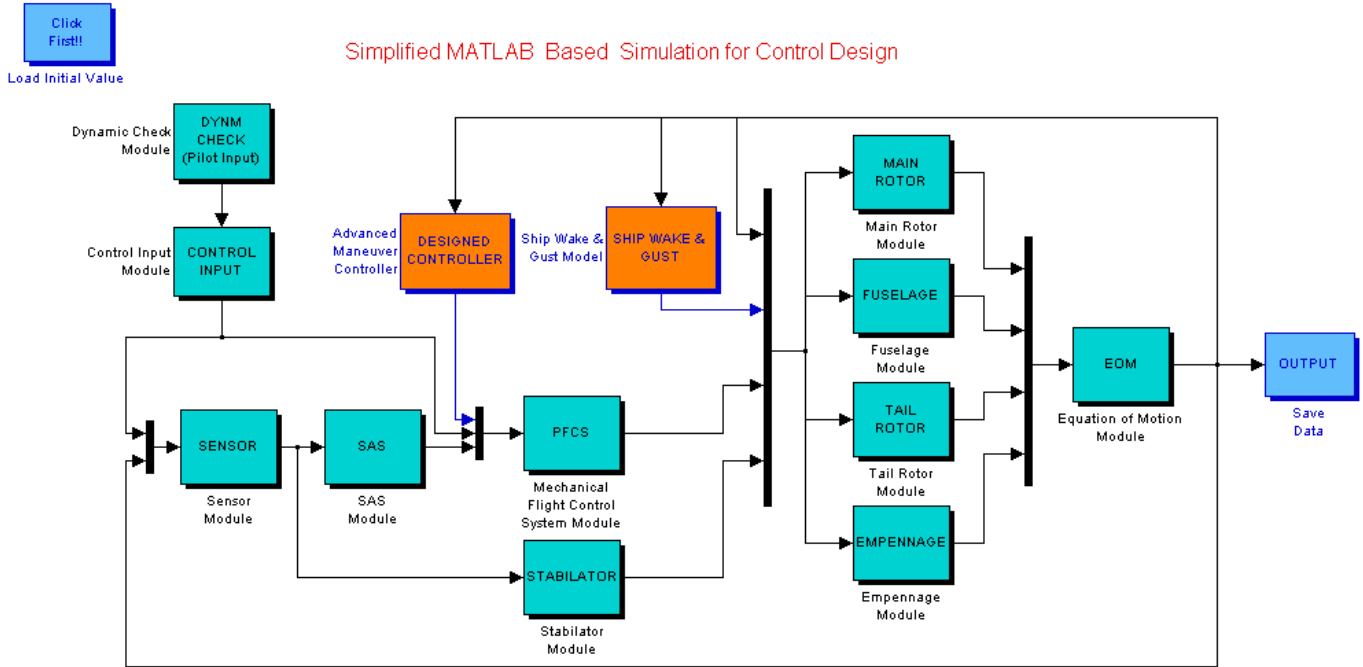


Figure 1. MATLAB/SIMULINK based simulation model

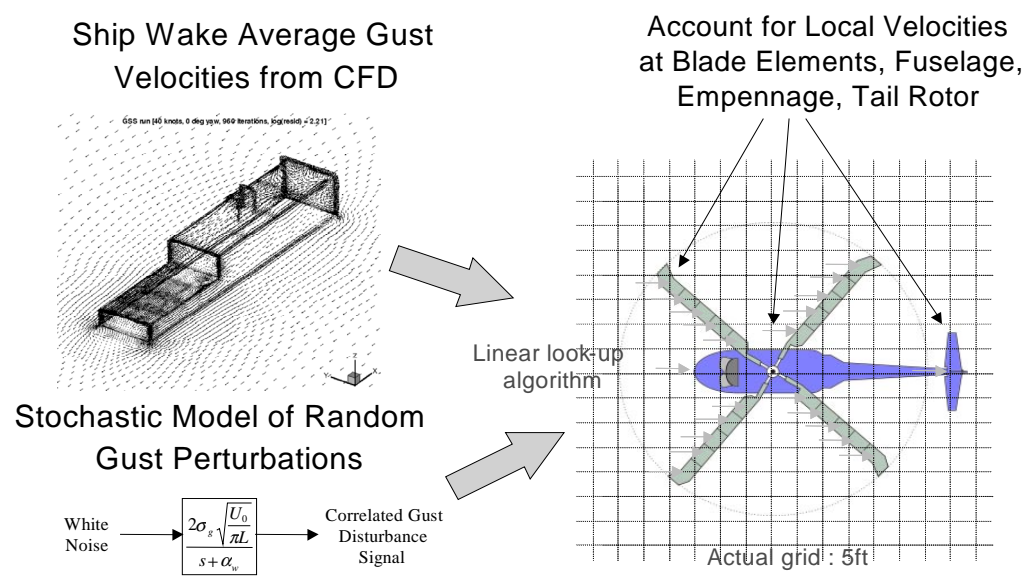


Figure 2. Gust penetration model

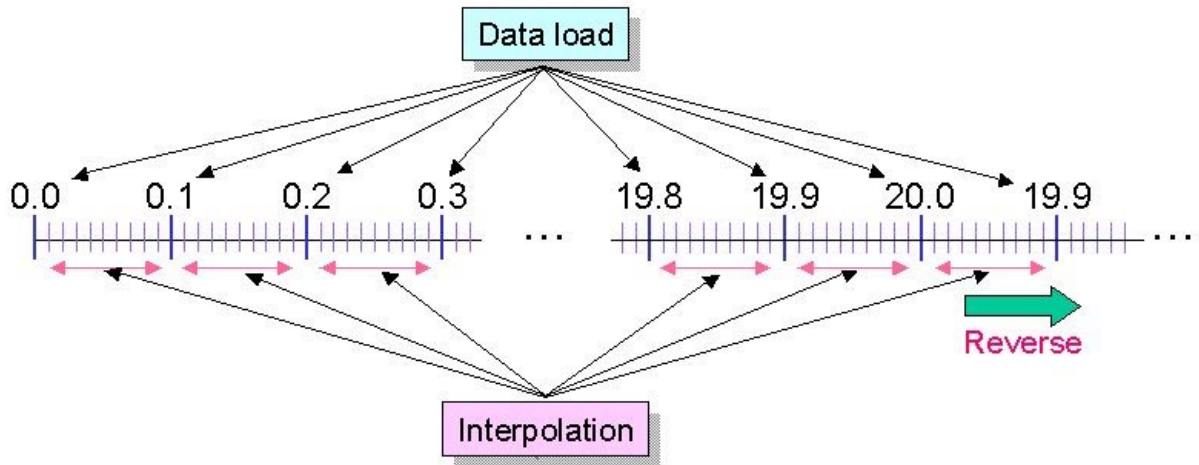


Figure 3. Interpolation algorithm for time-varying airwake

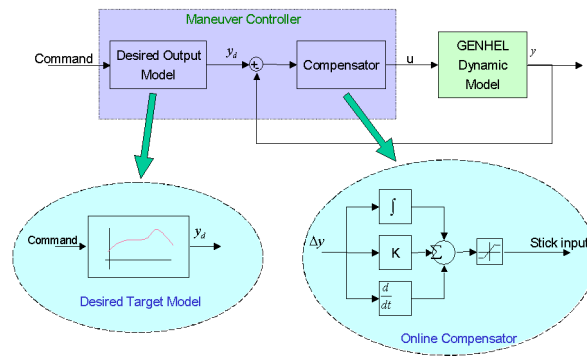


Figure 4. Control system structure

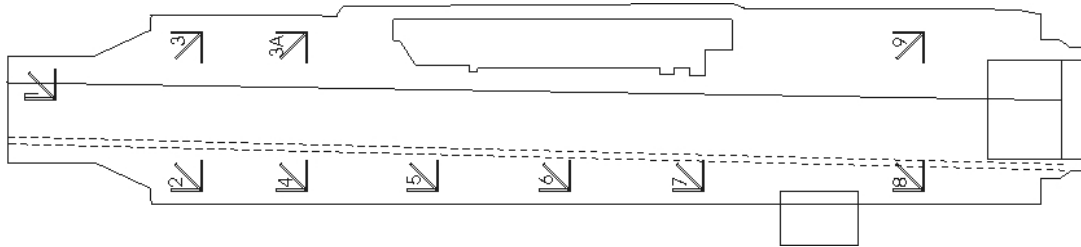


Figure 5. Top view of LHA class ship

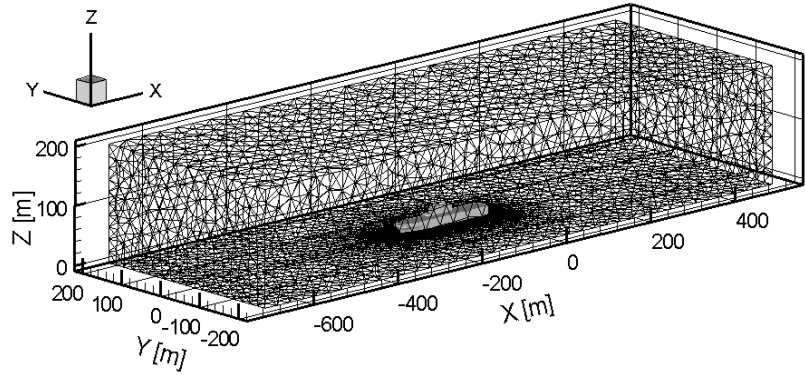


Figure 6. Unstructured grid domain around the LHA.

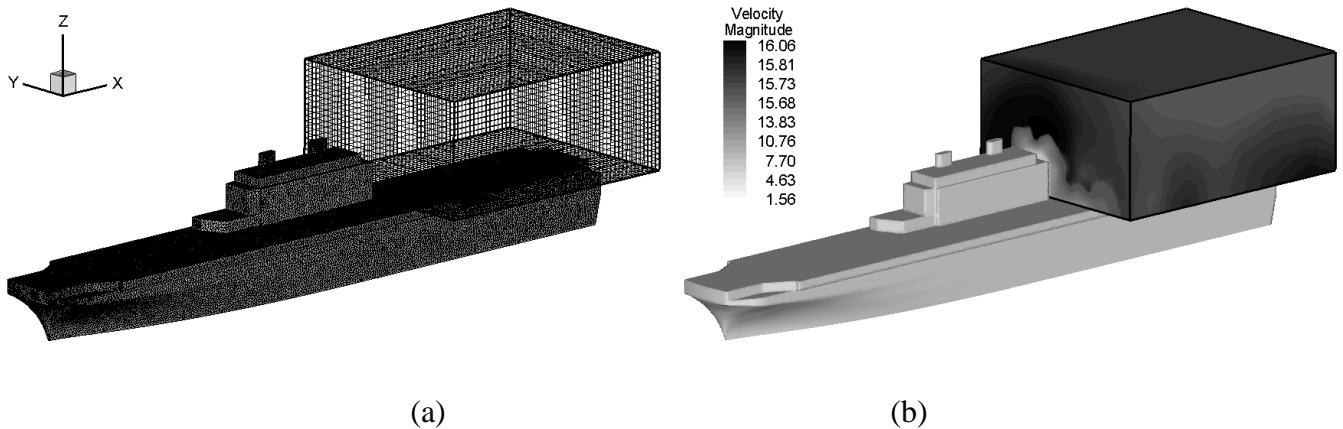


Figure 7. a)Rectangular volumetric domain of CFD data at the rear deck of LHA for DI simulations b)Velocity magnitude contours on the boundaries of DI mesh

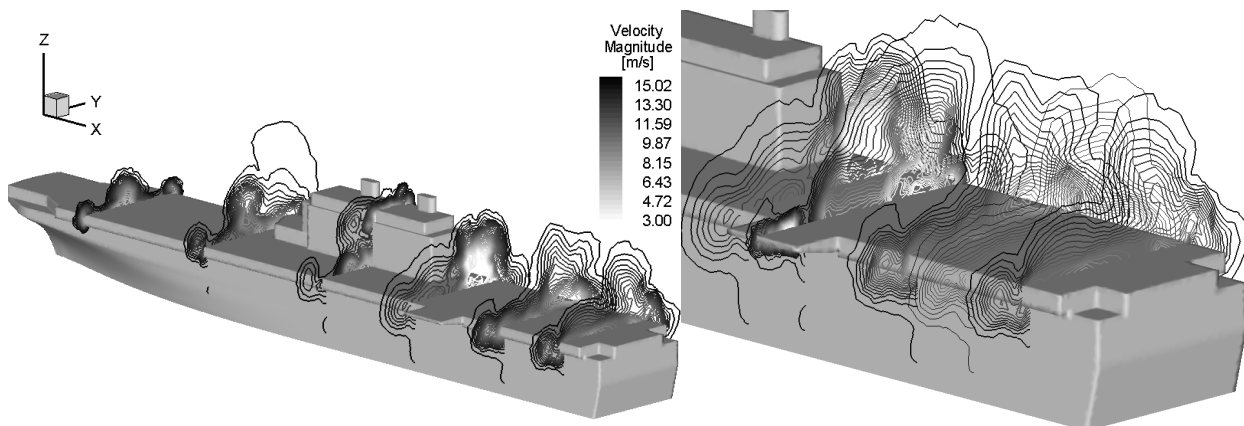


Figure 8. Velocity magnitude contours at several y-z planes over LHA at $t = 20$ seconds

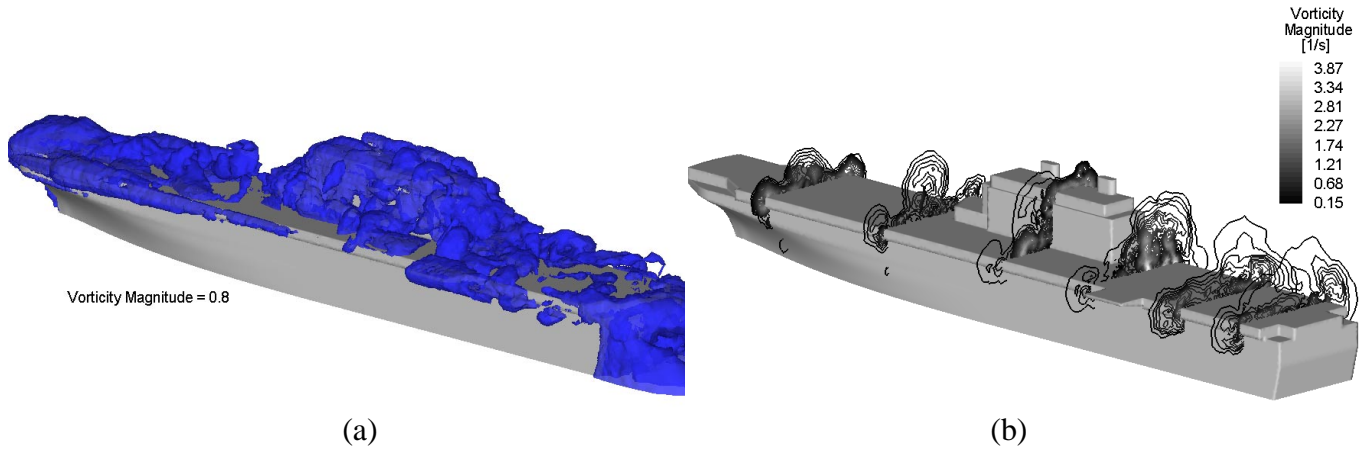


Figure 9. a) Vorticity magnitude iso-surface and b) Vorticity magnitude contours at several y-z planes over LHA at $t = 20$ seconds

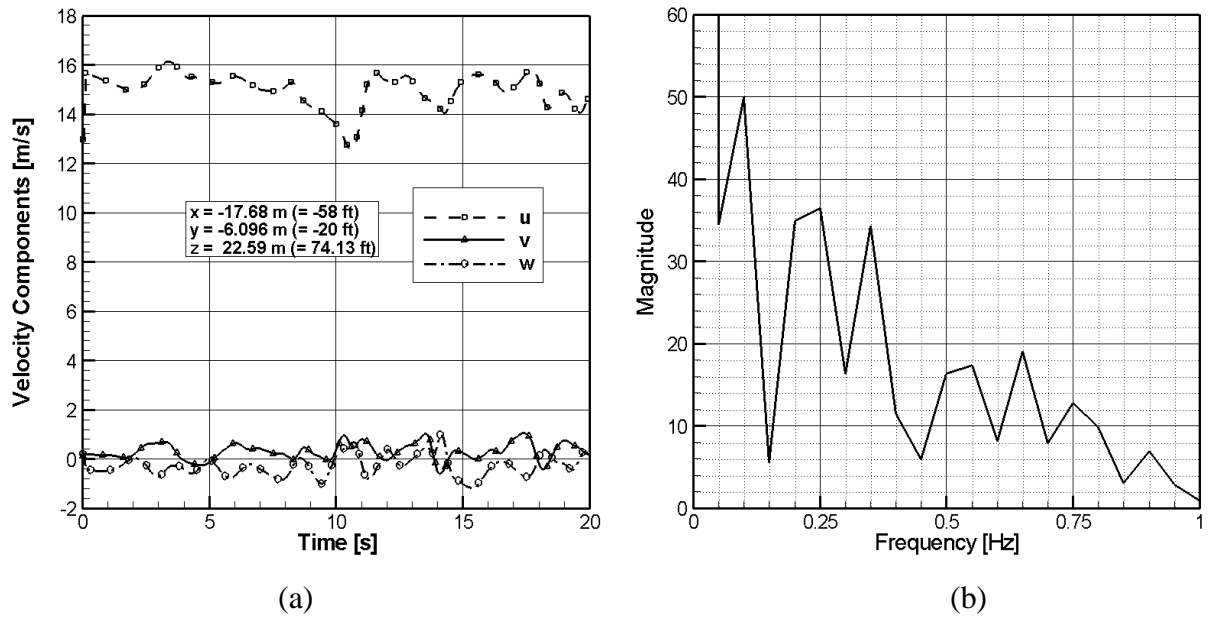


Figure 10. a) Time histories of u, v, w velocity components at a selected point in the DI mesh for the CFD data. b) Frequency spectrum of velocity magnitude of CFD data

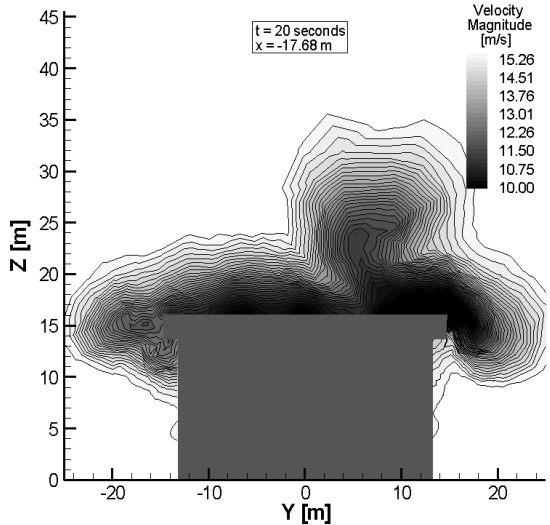
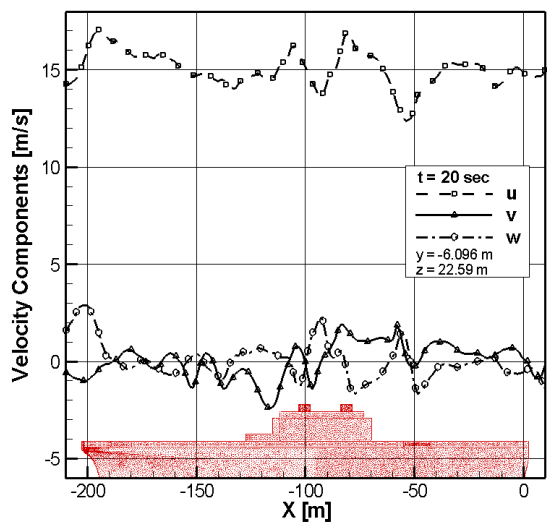
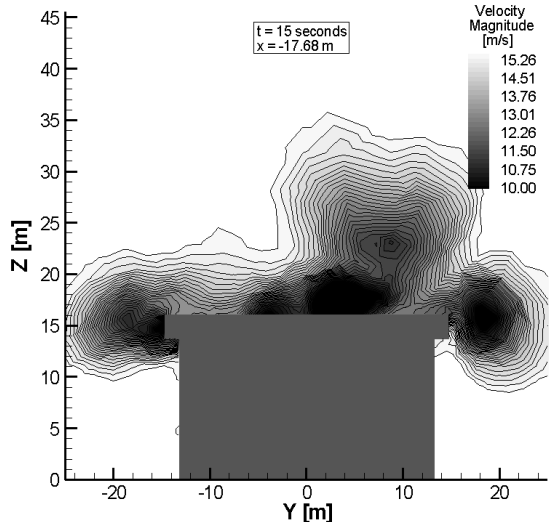
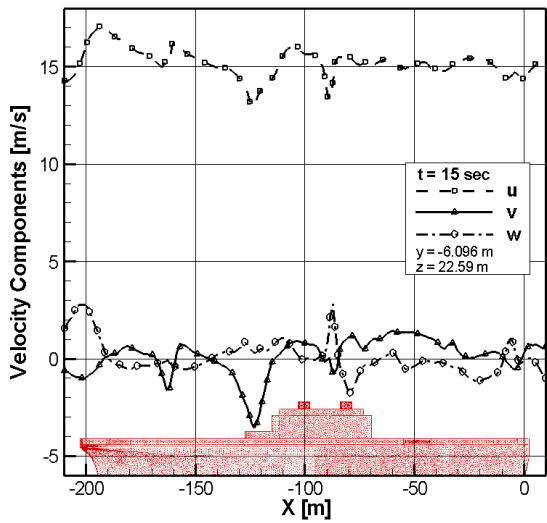
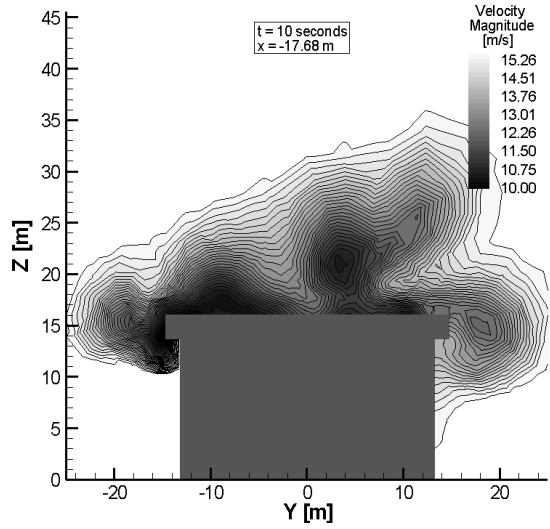
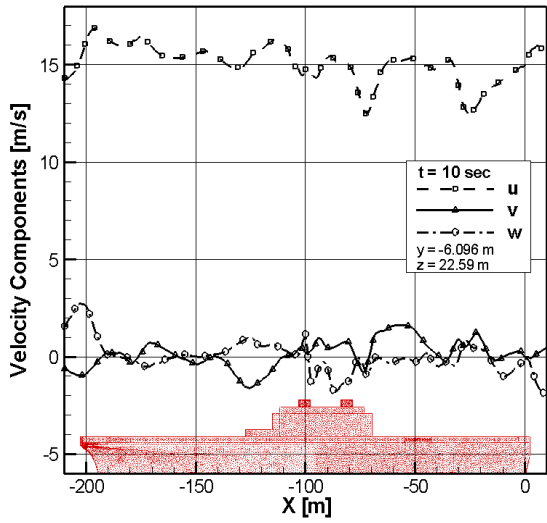


Figure 11. a) Distribution of velocity components along the length of LHA at $z = 22.59$ m and b) Velocity magnitude contours at $x = -17.68$ m for simulation times of 10, 15, 20 seconds.

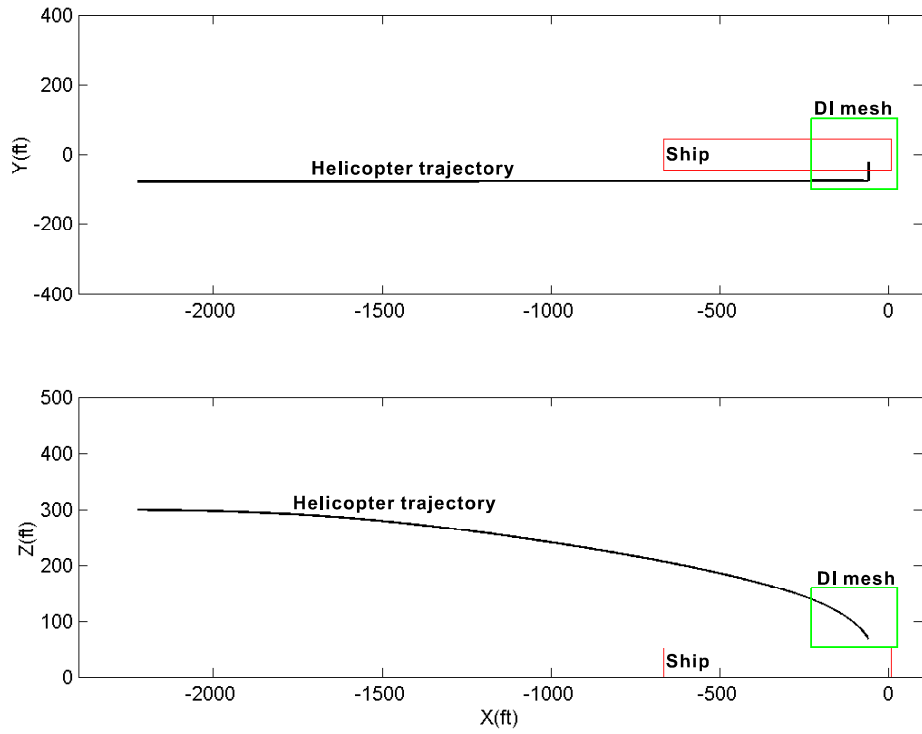


Figure 12. Helicopter position (ft) w.r.t. ship coordinate system – Departure case

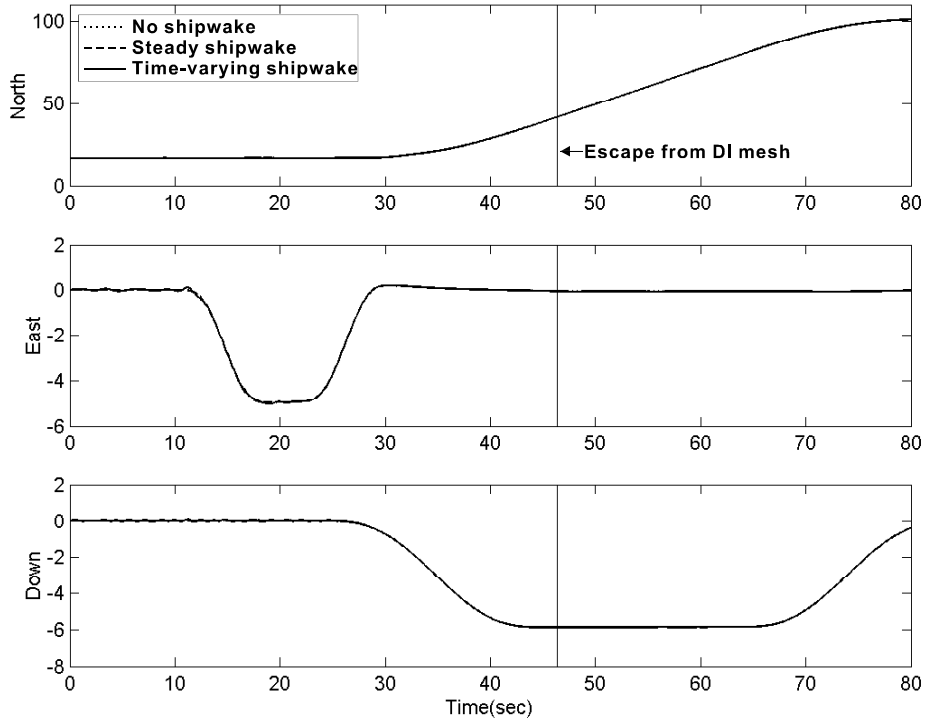


Figure 13. Helicopter velocity (ft/sec) vs. time (sec) – Departure case

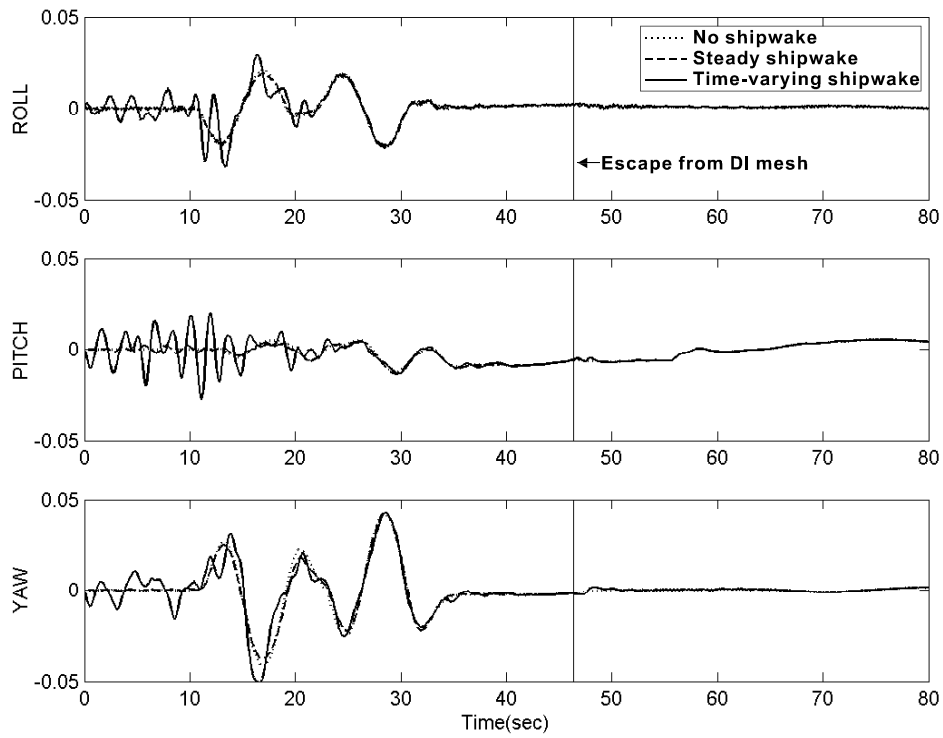


Figure 14. Helicopter angular rate (rad/sec) vs. time (sec) – Departure case

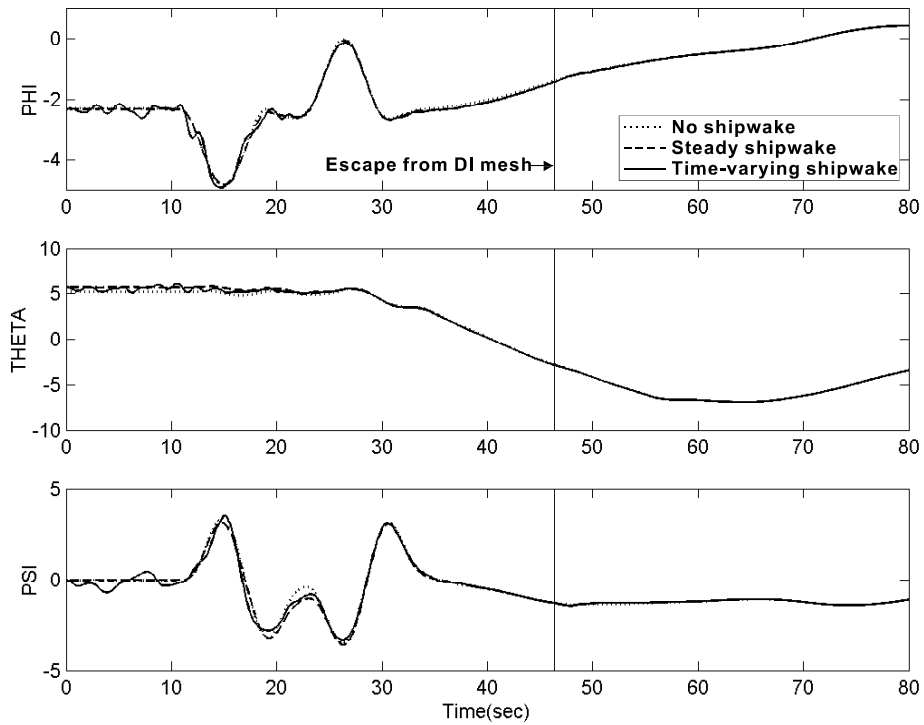


Figure 15. Helicopter attitude (deg) vs. time (sec) – Departure case

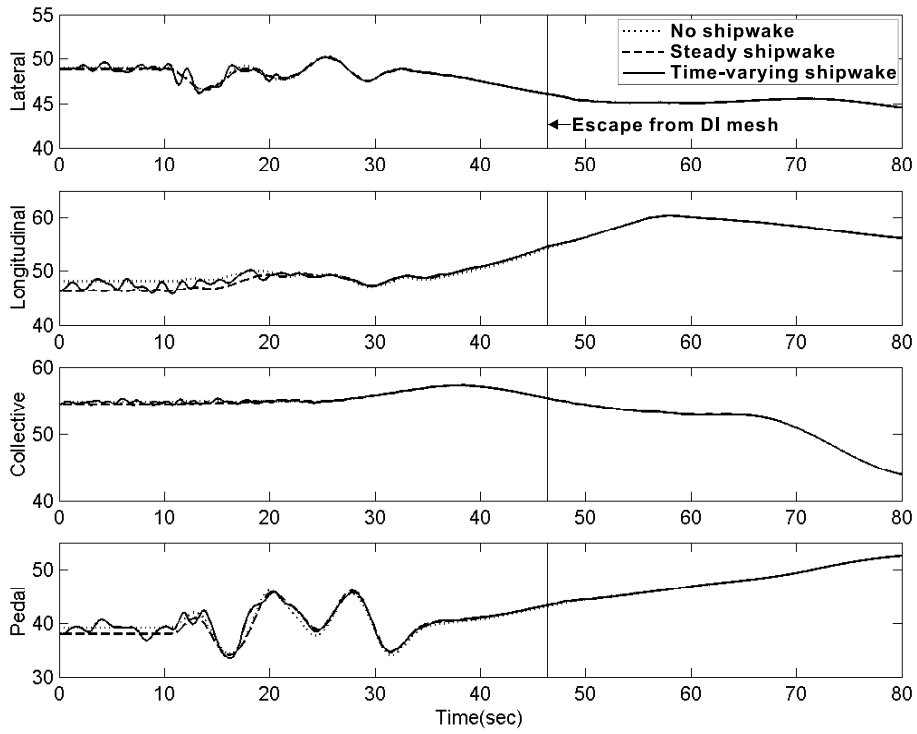


Figure 16. Pilot input (%) vs. time (sec) – Departure case

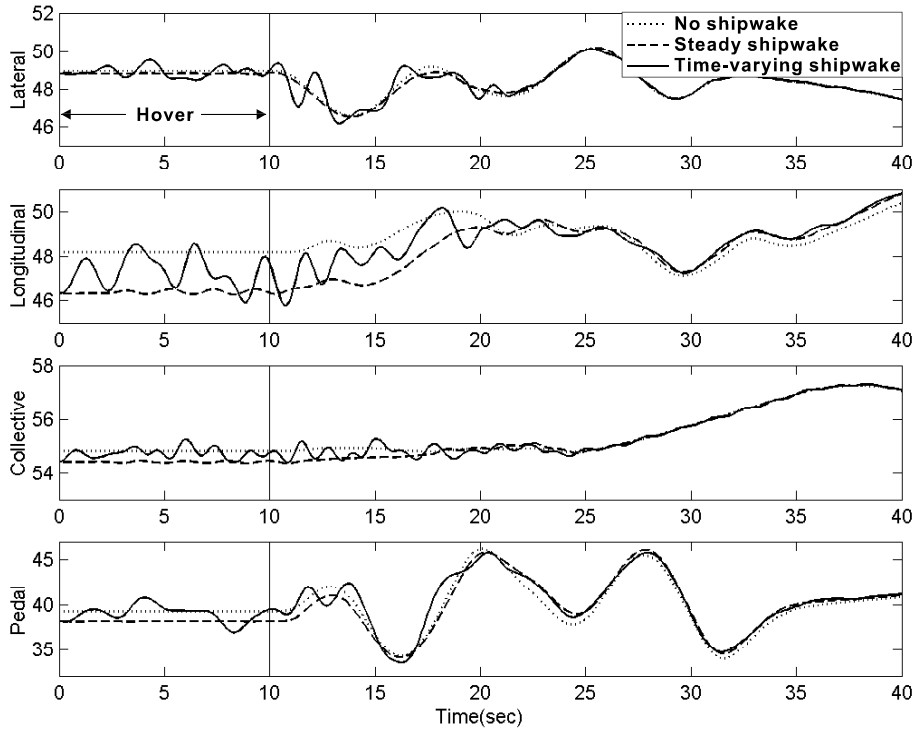


Figure 17. Pilot input (%) in 0 ~ 40 seconds – Departure case

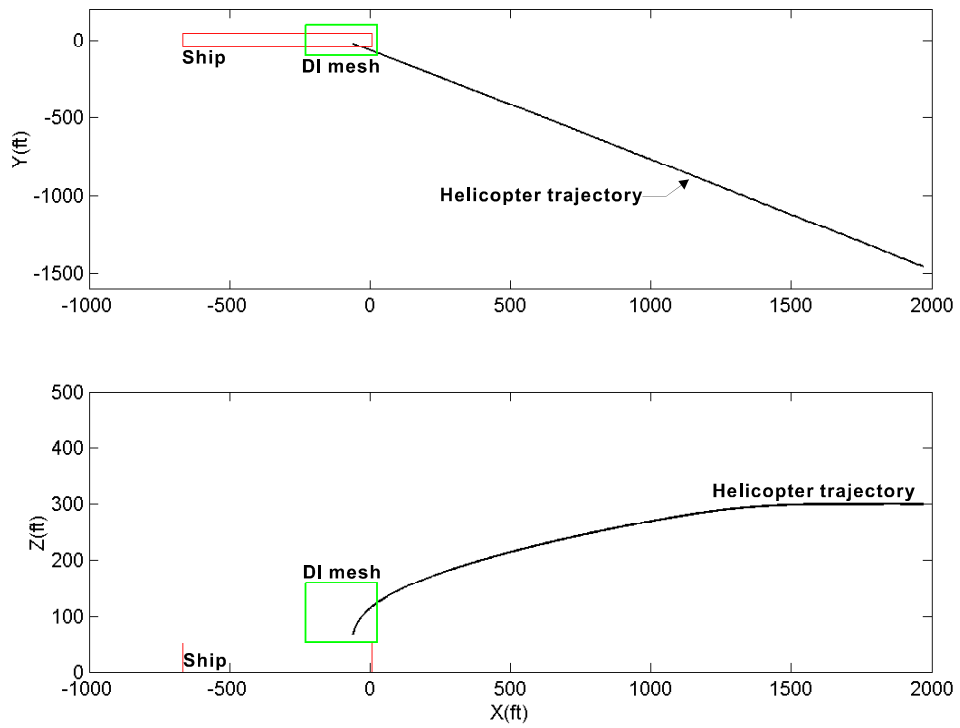


Figure 18. Helicopter position w.r.t. ship coordinate system (ft) – Approach case

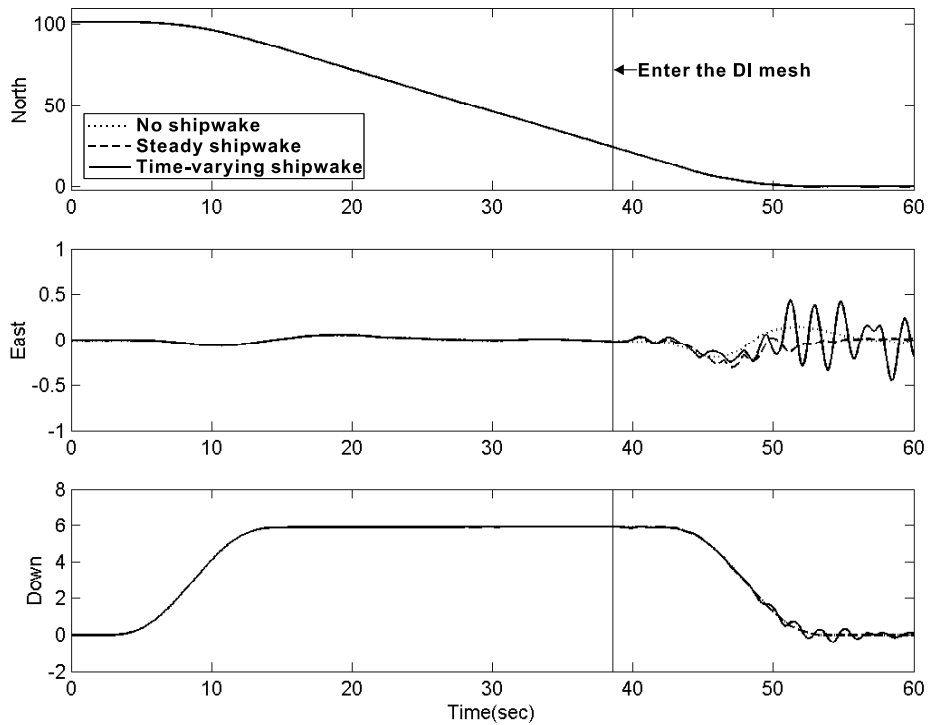


Figure 19. Helicopter velocity (ft/sec) vs. time (sec) – Approach case

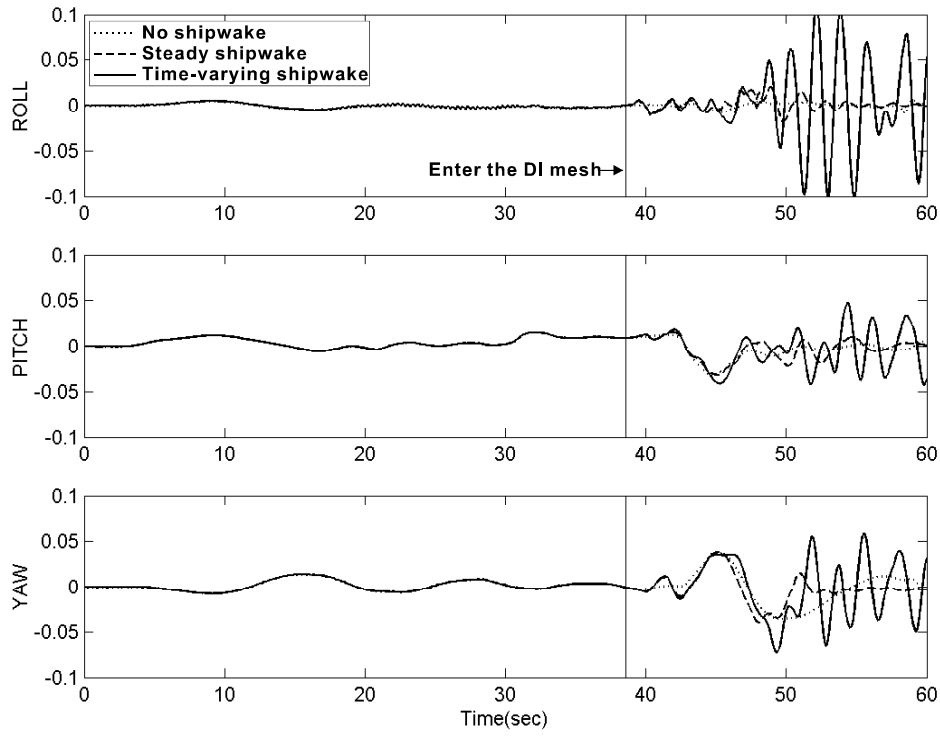


Figure 20. Helicopter angular rate (rad/sec) vs. time(sec) – Approach case

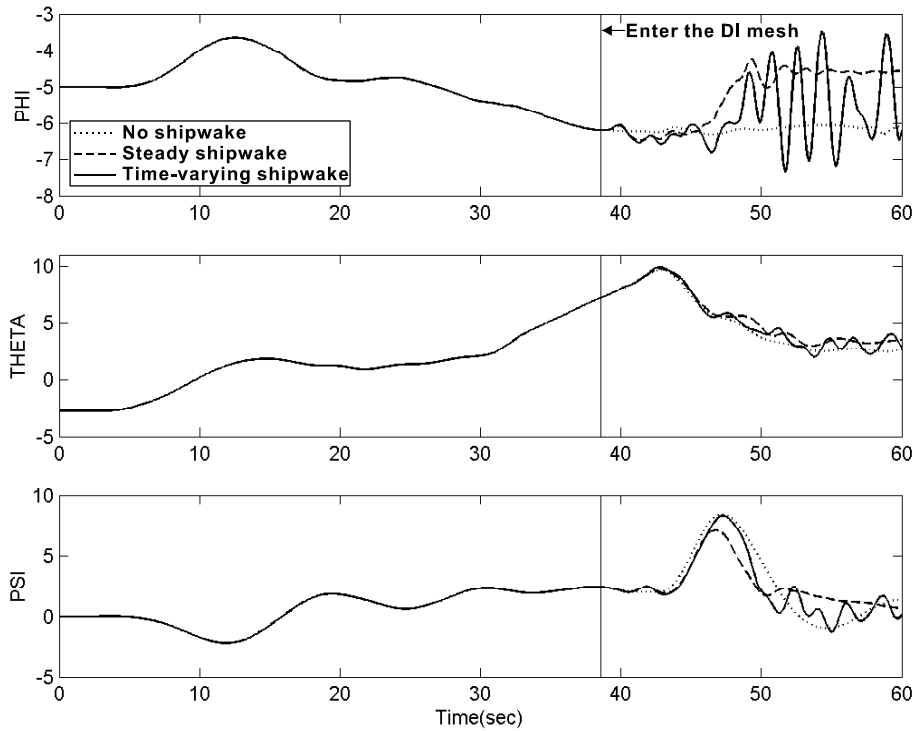


Figure 21. Helicopter attitude angle (deg) vs. time (sec) – Approach case

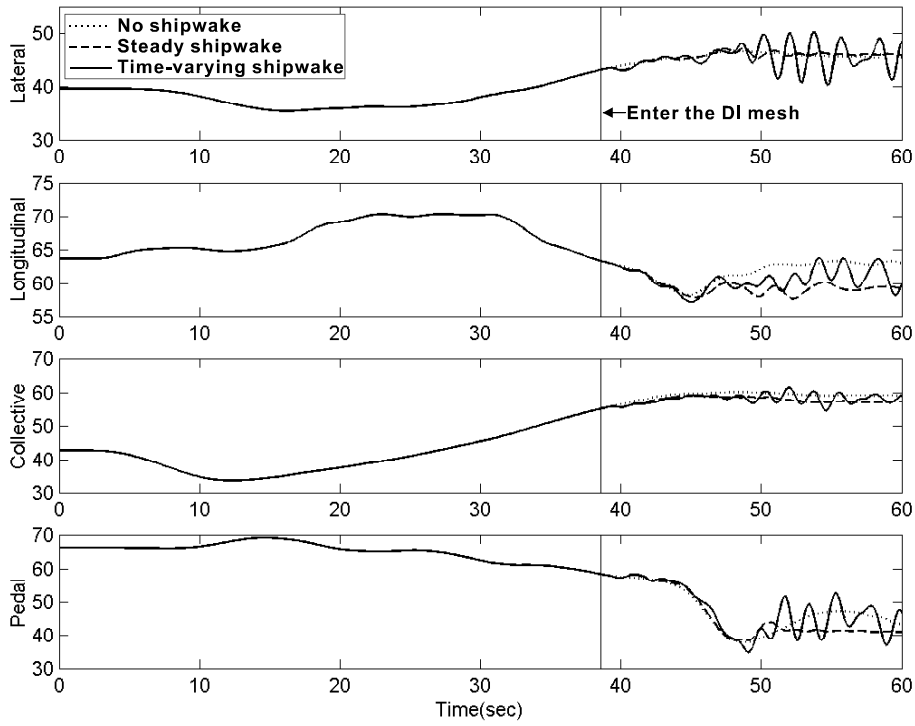


Figure 22. Pilot input (%) vs. time(sec) – Approach case

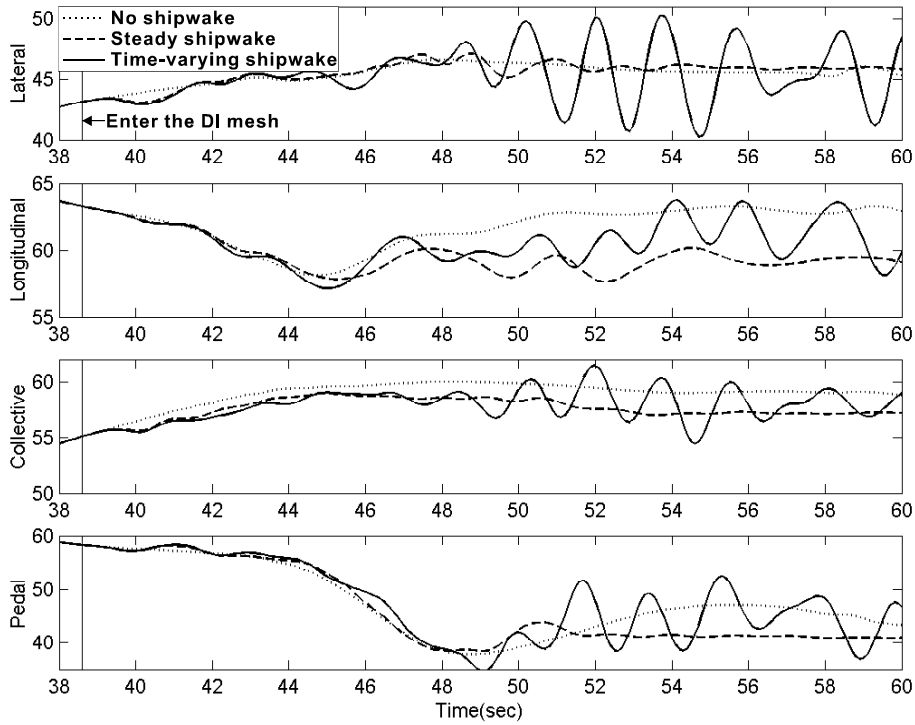


Figure 23. Pilot input (%) after entering the DI mesh – Approach case